Journal of Photochemistry & Photobiology A: Chemistry 373 (2019) 162–170

Contents lists available at ScienceDirect

Journal of Photochemistry & Photobiology A: Chemistry

journal homepage: www.elsevier.com/locate/jphotochem

Paracetamol mineralization by Photo Fenton process catalyzed by a Cu/Fe-PILC under circumneutral pH conditions

Lourdes Hurtado[a], Rubi Romero[a,*], Arisbeht Mendoza[a], Sharon Brewer[b], Kingsley Donkor[b], Rosa M. Gómez-Espinosa[a], Reyna Natividad[a,*]

[a] Centro Conjunto de Investigación en Química Sustentable, UAEMex-UNAM, Universidad Autonoma del Estado de Mexico, km 14.5 Carretera Toluca-Atlacomulco, 50200, Toluca, Mexico

[b] Department of Chemistry, Faculty of Science, Thompson Rivers University, Box 3010, 900 McGill Road, V2C 5N3, Kamloops, B.C., Canada

ARTICLE INFO

Keywords:
Pillared clays
Paracetamol
Photo-Fenton

ABSTRACT

This study presents an iron-pillared clay (Fe-PILC) ion-exchanged with copper (Cu/Fe-PILC), as an efficient catalyst to conduct the mineralization of paracetamol through photo-Fenton process at near to neutral pH without precipitation of Fe complexes and without adding any chemicals to modify the initial pH. The specific surface area of the catalyst was of 110 $m^2 g^{-1}$ and with the following phases FeO, Fe_3O_4, Cu_2O, CuO determined by XPS analyses. Around 80% of mineralization was reached either by conducting the process at acidic and circumneutral pH conditions, and the efficiency was not significantly higher at pH = 2.7. The intermediate reaction products generated at both pH conditions essayed and detected by LC–MS were hydroquinone, acetamide and oxamic acid. Catalyst Cu/Fe-PILC showed an iron leaching of about 3% after reaction while the reusability of the catalyst involved a decrease in mineralization of only 3% under circumneutral conditions. The final TOC of about 20% can be ascribed to the presence of acetamide that was found to be the most reluctant towards oxidation.

1. Introduction

Nowadays, the extended use of painkillers by people around the world is a real concern for environment. Among this group of drugs, non-steroidal anti-inflammatory drugs (NSAIDs) have been receiving increasing attention due to the toxic metabolites released to the environment produced by their degradation [1]. Paracetamol, also known as acetaminophen, is classified as a NSAID of wide use due to its accessibility without prescription. From the point of view of toxicity, the degradation products of paracetamol are potentially toxic implying cellular damage, inhibition of reproduction or even, death of species [2,3]. Several effluent treatments have been studied to efficiently destroy this molecule and its intermediate products, among them, advanced oxidation processes including photolysis [4], heterogeneous photocatalysis [5,6], electro-Fenton [7,8] and photo-Fenton [9]. Fenton is considered as an advanced oxidation process that combines ferrous ions and hydrogen peroxide (H_2O_2) to promote the generation of the hydroxyl radicals in aqueous solution. In order to enhance the degradation of organic pollutants, external sources of energy have been added to the Fenton process including UV light (photo-Fenton process), electricity (electro-Fenton process) and ultrasound (Sono Fenton Process) [10]. The simplified chemical reactions involved in a photo-Fenton process are below presented [11],

$$Fe^{3+} + h\upsilon \rightarrow Fe^{2+} + HO\bullet + H^{+} \quad (1)$$

$$Fe^{2+} + H_2O_2 \rightarrow Fe^{3+} + HO\bullet + OH^{-} \quad (2)$$

$$\bullet OH + organic\ pollutants \rightarrow oxidized\ products \quad (3)$$

Some important advantages of employing photo-Fenton processes have been reported by Nidheesh [10] in a very complete review about Fenton processes, including: i) the additional generation of hydroxyl radicals by decomposition of H_2O_2; ii) the rapid generation of ferrous ions in the presence of UV light and iii) the decrease in the amount of iron sludge formation compared to the Fenton process. A drawback of Fenton processes in general, is the necessity of acidic conditions to avoid precipitation of iron complexes. This situation is impractical because in most of the cases, the pH of wastewaters is neutral or alkaline. In homogeneous processes, the performance of the photo-Fenton processes at pH higher than 3 is negatively affected and this behavior has been explained on the basis of an accelerated decomposition of H_2O_2 to water and oxygen, the diminishing oxidation potential of $^{\bullet}OH$ radicals and the precipitation of ferric hydroxide [12]. This important limitation

* Corresponding authors.
E-mail addresses: rromeror@uaemex.mx (R. Romero), rnatividadr@uaemex.mx (R. Natividad).

https://doi.org/10.1016/j.jphotochem.2019.01.012
Received 20 September 2018; Received in revised form 16 December 2018; Accepted 13 January 2019
Available online 14 January 2019
1010-6030/

for the photo-Fenton process imposed by the narrow pH interval (close to 3) required for good performance has been given attention by various research groups [13–15]. An interesting strategy is to prevent iron precipitation in photo-Fenton in homogeneous phase by addition of iron complexing agents to the reaction media, among them citrate and oxalate [16,17]. This procedure allows the strongly complexing Fe(III) ions to form stable species and prevent Fe(III) precipitation as hydroxide.

When photo-Fenton processes can be conducted in homogeneous phase exhibiting and obtaining good results in terms of mineralization, the separation of the catalyst from the reaction media is difficult. This problem is solved by carrying out the process in heterogeneous media. In addition to the advantage of easy separation of the catalysts at the end of the process, in a heterogeneous system, iron is immobilized and Fe^{3+} species cannot be easily transformed into less photoactive materials like $Fe(OH)_3$ at pH higher than 3.0 [18]. In homogeneous systems, the opposite situation may easily occur. Thus, numerous catalysts have been studied as the source of iron for Fenton processes but among them pillared clays are receiving growing attention in the field [19–21]. A clay is defined as a fine-grained soil which contain minerals (including phyllosilicates of iron, magnesium, alkali metals, alkaline earth metals, etc.) and possesses a layered structure of silicate sheets bonded to aluminum oxide/hydroxide sheets [22]. The interest of employing clays as catalysts in photo-Fenton processes is given by their low cost, availability, and inexistent toxicity. However the content of iron in natural form in clays is considerably low for a successful application in Fenton reactions, so to overcome this difficulty, several methods have been tested to increase the content of iron in clays: cation exchange, impregnation methods and pillaring [23]. The pillaring of a clay with metallic species normally includes the polymerization of a multivalent cation, followed by its intercalation into the interlayer space of the clay and a final thermal treatment to give a fixed metal oxide pillar with high thermal stability and large surface area as resultant product [24].

Clays already have been employed as catalysts in photo-Fenton process at pH higher than 3.0, for example in the Orange II discoloration and mineralization employing bentonite and laponite [25] as well as in the degradation of Acid Black 1 using a modified laponite clay-based Fe nanocomposite [26] among others. In these reports, the degradation experiments were conducted at pH of the solution close to neutral observing reasonably good performance and negligible iron leaching. Another strategy to produce functionalized catalysts to conduct efficient photo-Fenton process in a wide pH interval is to include in the structure different cations additionally to the iron species. In this sense, it has been stated that copper exhibits less sensitivity than iron to changes in pH and this fact represents a promising alternative to conduct photo-Fenton processes in a wide pH intervals maintaining good photocatalytic activity [27].

The use of Cu-PILC as catalyst of the Fenton-like process has been mainly studied without the use of light [28–33]. In some of these studies, Cu has been added to already pillared clays with Fe and Al. Within these studies, it has been demonstrated that the addition of Cu benefits the organic compounds oxidation, and this is ascribed to a synergism between Cu and Fe. It has been concluded [30] that in addition to typical Fenton reaction (Eq. (2)), there are other species that might be appearing, like the reactive intermediate $\equiv Cu^{2+} - OH^{\cdot}$, that contribute to organic compounds degradation. Specifically, during paracetamol degradation, it has also been recently demonstrated [34] that Cu^{+} activates oxygen to produce powerful reactive oxygen species (H_2O_2, $^{\cdot}O_2^-$ and $^{\cdot}OH$).

Thus, because all the aforesaid, this work aimed to synthesize, characterize and assess the performance of a Cu/Fe-pillared clay to achieve the efficient abatement of paracetamol molecule by photo-Fenton process at other than acidic pH conditions.

2. Materials and methods

2.1. Reagents

Pillared clays were prepared from Bentonite (pure-grade) supplied by Fisher Scientific. Sodium hydroxide (NaOH), Ferric chloride hexahydrate ($FeCl_3{\cdot}6H_2O$, 99%) and hydrochloric acid (HCl, 37%) were employed in the synthesis of pillared clays and purchased from Fermont. Copper (II) acetate monohydrate ($Cu(CH_3COO)_2{\cdot}H_2O$, 0.5 M) was provided by J.T. Baker. Sulfuric acid (H_2SO_4, 96.9%) and hydrogen peroxide (30%), supplied by Fermont were used to conduct the Photo-Fenton process. Acetaminophen ($C_8H_9NO_2$, 98%, MW: 151.17, mp: 168–172 °C, ρ: 1.293 g ml^{-1}) was purchased from Alfa Aesar.

2.2. Catalysts synthesis

2.2.1. Fe-PILC´s preparation

Iron pillared clays (Fe-PILC's) preparation starts with the pillaring solution preparation, according to previously reported methods [35], as follows: 0.3 L of an aqueous solution of $FeCl_3{\cdot}6H_2O$ was slowly added to 0.6 L of 0.2 M NaOH aqueous solution at room temperature under continuous stirring; the resulting mixture was stirred for further 4 h at pH of 1.7 adjusted by HCl 5 M. After that, the pillaring solution was dropwise added to 0.1%wt aqueous bentonite suspension. The mixture was then kept under continuous stirring over 12 h. The next step was the recovery of the prepared powder by centrifugation for further chloride ions elimination by washing with deionized water until conductivity reached 5 μS/cm. The resulting powder was dried overnight at 74 °C and calcined at 400 °C for 2 h.

2.2.2. Cu-Fe- PILC's synthesis

Once Fe-PILC's were obtained, the copper was introduced by ion-exchange. To achieve this, 0.1 L of 0.5 M $Cu(CH_3COO)_2{\cdot}H_2O$ were prepared per each gram of Fe-PILC obtained in the previous step. Finally, Cu/Fe-PILC's were calcined at 400 °C during 2 h.

2.3. Catalyst characterization

Structural, chemical and textural characterization of Cu/
Fe-PILC´s were performed by X-ray diffraction (XRD), Atomic absorption spectroscopy (AAS), Nitrogen physisorption and X-ray photoelectron spectroscopy (XPS). XRD patterns were obtained in a Bruker Advance 8 instrument using Cu-Kα radiation at 35 kV and 30 mA. The Fe and Cu content (wt%) was determined by AAS, and for this purpose an AA240FS VARIAN spectrometer was employed. Samples were dissolved in hydrofluoric acid and diluted down to the interval of measurement. Specific surface area was determined by BET methodology from data of N_2 physisorption performed in an Autosorb-1 analyzer from Quantachrome instruments; samples were degassed during 2 h prior to adsorption measurements. XPS measurements were carried out in a JEOL spectrometer (Model JPS-9010) with base vacuum in the analysis chamber of 10^{-8} Pa and 30 scans. The X-ray photoelectron spectra were recorded with Mg Kα excitation source with photon energy of 1253.6 eV.

2.4. Paracetamol degradation

Paracetamol degradation by photo-Fenton experiments were conducted in a Pyrex glass reactor (dimensions: 20 cm length, 2.5 cm diameter) containing 0.1 L of an aqueous solution of paracetamol (C_0 = 100 ppm). Temperature of the reaction system was kept at 298 K and it was controlled by a thermal bath. The light source was an 8 W high-pressure mercury lamp (UVP-Pen Ray Model 3SC-9) that provides radiation at 254 nm and was placed inside the reactor at the central axis. Stirring was provided at 800 rpm during the entire experiment. In a typical experiment, the paracetamol solution was placed inside the

reactor followed by the dispersion of 50 mg of the catalyst; after that if the experiment required acidic conditions, the pH was adjusted with 0.1 M H_2SO_4 followed by simultaneous starting of illumination and addition of a stoichiometric amount of H_2O_2 (145 μL) to the system. The previous conditions were established as optimal in a separate study not included here [36]. Samples were periodically withdrawn to determine paracetamol and by-products time evolution as well as percent of mineralization reached. For this purpose, High Performance Liquid Chromatography coupled to Mass Spectroscopy (HPLC-MS) and Total Organic Carbon (TOC) analyses were conducted.

HPLC-MS analyses were carried out in an Agilent 1200 series HPLC system (Agilent Technologies, Mississauga, ON, Canada) coupled to an Agilent 6530 Accurate-Mass Quadrupole Time-of-Flight (Q-TOF) spectrometer equipped with electrospray ionization (ESI) source (gas temperature, 350 °C; drying gas, 13 L min^{-1}; nebulizer, 60 psig; sheath gas temperature, 325 °C; sheath gas flow, 12 L min^{1}; Vcap, 3500 V; fragmentor voltage, 60 V). Samples were analyzed in positive ion mode, and mass spectra were collected between 30 and 500 *m/z*. A sample volume of 2 μL was injected to the LC, and the flow rate was set to 0.4 mL min^{-1}. Separation was achieved in an Agilent Eclipse plus-C18 column (100 mm × 2.1 mm; 1.8-μm particle size; Agilent, Canada) kept at constant temperature of 35 ± 0.2 °C. Mobile phase (A) was composed of water with 1% formic acid; mobile phase (B) was composed of acetonitrile with 1% formic acid. Gradient elution was programmed as follows: 80% B at 0 min, decreased 60% - 30% at 3–5 min, increased 60% in 30 s, held at 80% at 5.50–6.0 min.

Paracetamol mineralization degree at different times of the photocatalytic process was established by direct determination of Total Organic Carbon (TOC) measured with a Shimadzu TOC-V_{CSH} instrument with an integrated Shimadzu ASI-V autosampler after acidification and sparging to remove the inorganic carbon. For both analyses, HPLC and TOC, the error was established to be lower than 2%.

3. Results and discussion

3.1. X-ray diffraction

A typical X-ray diffraction pattern of Cu-Fe-pillared clay is depicted in Fig. 1. In previous works [37,38], the DRX pattern of Fe-PILC was analyzed. In these studies, two main signals were identified; one of them located at 4° and the other one between 7° and 9° in 2θ. The second peak is characteristic of the raw clay (bentonite) at 9° and has been assigned to the basal (0 0 1) reflection ($d_{0\ 0\ 1}$) related to the distance between interlaminar layers of the bentonite (XRD pattern not shown in this work). The introduction of Fe polycations into the interlayer spaces of the bentonite causes the sheets to separate by approx.

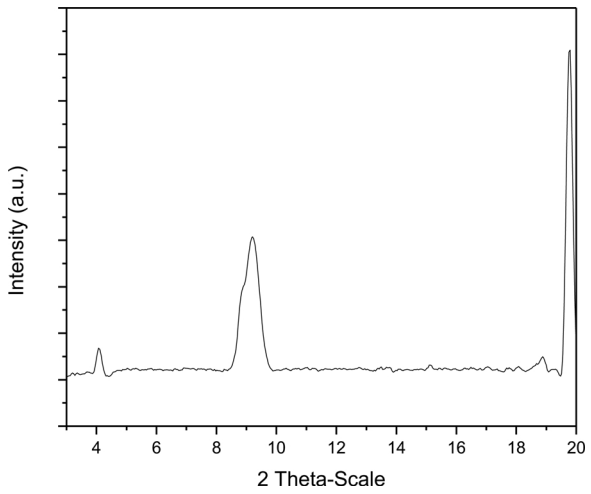

Fig. 1. XRD pattern of synthesized Cu/Fe-PILC.

12 Å (21.432 Å corresponding to ($d_{0\ 0\ 1}$) minus 9.6 Å corresponding to the thickness of the layers). Aforementioned, this peak appeared at smaller 2θ angles (2θ ≈ 4°). The signal at 20° has been reported as a quartz impurity in bentonite [39]. Dorado [40] have reported the presence of an angular reflection at 4° which is also observed in our pattern and can be ascribed to the enlargement of the interlayer space provoked by the pillaring process.

Regarding to the XRD pattern of Cu/Fe-pillared clay, this exhibited two peaks at 2θ about 4° and 9° similar to the peaks of Fe-PILC. The basal (0 0 1) reflection for Cu/Fe-PILC was $d_{0\ 0\ 1}$ = 21.438 Å (at 2θ ≈ 4°). Addition of Cu did not affect the structure of Fe-PILC.

3.2. XPS

Analysis of the Fe-PILC and Cu/Fe-PILC samples by X-ray photoelectronic spectroscopy helped to determine the oxidation states of the metals and the generated spectra are presented in Fig. 2. In Fig. 2 depicts Fe $2p_{1/2}$, Fe $2p_{3/2}$, Cu $2p_{1/2}$ and Cu $2p_{3/2}$ spectra. After deconvolution the presence of ferrous oxide (709.6 eV and 722.4 eV), ferrous ferric oxide (710. 4 eV and 723.4 eV), cuprous oxide (932.0 eV and 951.8 eV), cupric oxide (932.7 eV and 952.5 eV), were determined according to data provided by the National Institute of Standards and Technology (NIST). Fe_3O_4 (or magnetite) is an oxide of mixed valence (Fe^{2+}/Fe^{3+}). In a recent publication by Minella et al. [11], it is reported that magnetite has successfully been used as source of iron in Photo-Fenton process under circumneutral pH conditions and the importance of magnetite is the stability exhibited under a wide interval of pH in addition to the Fe^{2+}/Fe^{3+} ratio available to conduct reactions represented by Eqs. (1) and (2) for the production of a high proportion of hydroxyl radicals and, the capacity of reutilization without relevant losses in performance. In addition, it can also be noticed the absence of the signal corresponding to Fe_2O_3 which usually is appreciable in Fe-PILC's as reported by Martin del Campo et al. [37]. This result is consistent with a TPR study [41], where the Fe-PILC clay showed a reduction peak at 350–370 °C corresponding to the $Fe^{3+} \rightarrow Fe^{2+}$ reduction process. This fact, however should not reduce the photochemical performance of the catalyst since Fe^{2+} is considerably more reactive than Fe^{3+} towards H_2O_2 [11]. Regarding copper, cuprous oxide and cupric oxide were detected by XPS analysis. This result is in concordance with other works, that indicate the presence of Cu^{2+} and Cu^{+} in similar catalysts [28,41]. The cuprous oxide has been recognized as a promising material for environmental applications due to its low toxicity, low cost and good environmental acceptability and furthermore, its use in photochemical reactions is highly motivated for its small band gap (˜2.0 eV) which makes Cu_2O a suitable material to promote the utilization of visible light. On the other hand, however, it has also been reported that its activity is affected by the rapid recombination of electron-holes pairs [42,43].

3.3. Textural properties

The synthesized Fe-PILC and Cu/Fe-pillared clays exhibit a mesoporous surface given by their average pore diameter of 3.62 nm and 3.82 nm, respectively. Table 1 summarizes information about specific surface area, pore volume and metal content obtained for Cu/Fe-pillared clays and its comparison against raw clay. It is worth noticing the considerably increase in specific surface area and pore volume when bentonite is pillared. The incorporation of Fe to the raw clay structure results in an enhancement of both parameters, due mainly to microporous formation. Regarding to the formation of microporous and mesoporous under specific preparation conditions, it has been reported that micropores formation is given by the intercalation of smaller hydrolyzed iron oxides and in contrast, mesoporous appears when interparticle spaces are generated by coaggregation of iron polyoxocations on the clay mineral surface [5,44]. The introduction of copper by ion exchange to the Fe-PILC led to a decrease of the surface area and the

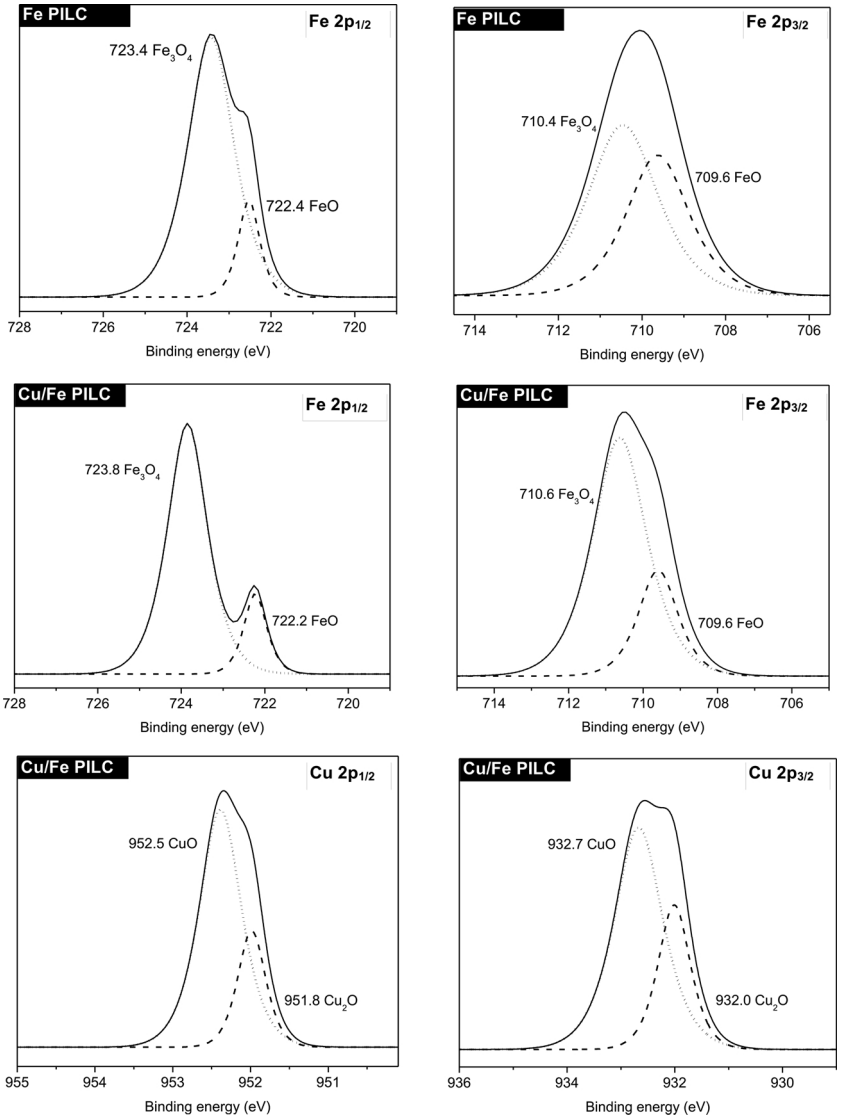

Fig. 2. Fe $2p_{1/2}$, Fe $2p_{3/2}$, Cu $2p_{1/2}$ and Cu $2p_{3/2}$ photoelectron spectra of Fe/PILC and Cu/Fe-PILC samples.

Table 1
Textural properties of the prepared clays and comparison with pure bentonite.

Material	Specific surface area ($m^2\,g^{-1}$)	Pore volume x 10^7 ($m^3\,g^{-1}$)	Metal content (wt.)
Bentonite	35	0.58	2.7 % Fe
Fe-PILC	283	1.85	16.72 % Fe
Cu/Fe-PILC	110	1.76	16.49% Fe 4.04% Cu

pore volume. This may be due to a partial blocking of the pillared matrix by the metal species located in the interlaminar areas [45]. Bahranowski suggested that the copper in the pillared matrix may be located at the following sites: (1) within the interlayer, with no strong bonds to either silicate sheet or pillars, (2) coordinated to the oxygens of the silicate layer, or (3) coordinated to a pillar [28,46]. A slight decrease in the iron content was observed after Fe-PILC was exchanged with copper. This result would indicate that the Na^+ ions, originally present in the Fe-PILC, have been ion exchanged by Cu^{2+}. This suggested that copper was introduced into the interlayer area.

The adsorption/desorption isotherms for the samples Fe-PILC and Cu/Fe-PILC are shown in Figure S1 as supplementary material. The isotherms shapes are type I(b) and IV(a) according to the International Union of Pure and Applied Chemistry (IUPAC) system [47]. The isotherms exhibited H3 hysteresis (IUPAC classification), this is characteristic of slit shape pores, typical in pillared clays, which indicates that the configuration of parallel plates of clay minerals is maintained [48].

3.4. Oxidation of paracetamol by photo-Fenton process catalyzed by Cu/Fe-PILC's

First of all, in order to ensure the efficiency of the photo-Fenton process, the following set of control experiments was conducted: photolysis (UV light and paracetamol) and adsorption (Cu/Fe-PILC). It was concluded that no paracetamol mineralization was appreciable by either of these processes.

Fig. 3 shows the normalized paracetamol concentration evolution with time during the photo-Fenton process at two pH, 2.7 and 5.8 with the synthesized catalysts. It can be observed that a total oxidation of paracetamol is achieved at both pH. Such oxidation is expected to occur mainly by a photo-Fenton process (Eqs. (1)–(3)) and similar reactions are expected to occur with Cu, i.e. photo-Fenton like process. The role of Cu, however, is expected to be beyond its participation in the production of OH radicals by catalyzing H_2O_2 dissociation. It has been demonstrated [34], albeit with radiation and Fe-free systems, that Cu

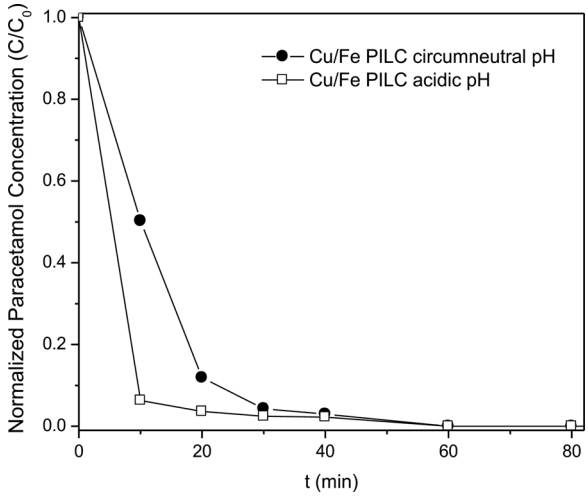

Fig. 3. Normalized paracetamol concentration profile. Effect of pH reaction conditions. Reaction conditions: $C_0 = 100\,mg\,L^{-1}$, rpm = 800, T = 298 K, $W_{cat} = 0.5\,g\,L^{-1}$, $V_{reaction} = 0.1\,L$.

also participates in the activation of oxygen and production of H_2O_2 by means of the following reaction,

$$Cu^{+} + O_2 + 2H^{+} \rightarrow Cu^{2+} + H_2O_2 \quad (4)$$

This reaction is favored under acidic conditions and is expected to favor the whole process not only by generating the H_2O_2 but also by reacting with O_2 and thus offering a "protection" to iron so this is not oxidized by this route. It has also been suggested [30] for Fe containing systems, albeit without light, that the role of Cu includes the generation of the reactive intermediate $\equiv Cu^{2+} - OH^{\cdot}$ (Eq. (5)) that is able to generate radicals from its reaction with aromatic compounds like phenol.

$$\equiv Cu^{+} + H_2O_2 \rightarrow \equiv Cu^{2+} - OH^{\cdot} + OH^{-} \quad (5)$$

The acetaminophen normalized concentration profiles shown in Fig. 3, suggest indeed that the generation of oxidant species is more effective at acidic pH since the initial oxidation rate when pH = 2.7 is 9.61×10^{-7} mol·L^{-1}·s^{-1} and is 5.47×10^{-7} mol L^{-1} s^{-1} at circumneutral pH. It is worth pointing out that during the entire experiment at circumneutral conditions, the pH was not adjusted allowing the natural curse of reaction and it was found that after three hours of process, the pH turned acidic (final pH equal to 4.5). This is likely due to the formation of carboxylic acids as product-sides and this will be discussed later in this manuscript. On the other hand, for the experiments under acidic conditions, it was necessary to periodically adding H_2SO_4 0.1 M to keep constant pH close to 3.0.

Although a strict comparison with results within literature is not possible because of the additional effect of the different employed reaction systems, i.e. initial paracetamol concentration, catalyst and type of reactor, Table 2 summarizes some initial paracetamol oxidation rates that were calculated from experimental data published within the cited references. It is worth pointing out that reports including the mixture of Cu and Fe were not identified within existing literature. It can be observed in Table 2, that despite the differences in the reaction systems, the paracetamol initial oxidation rate ($-r_{Po}$) is of the same order of magnitude for all elected systems. However, such rate becomes rather different when the number of active sites, directly proportional to the catalyst loading, is taken into account for such a calculation ($-r'_{Po}$). This rate per mass of catalyst is two orders of magnitude higher in our system than that calculated from photocatalysis data (TiO_2) and solar homogeneous Fenton ($FeSO_4$). The difference when using zero-valent copper only (Cu°) without light is even higher (up to 3 orders of magnitude). It is worth pointing out that, at any case, this cannot be considered as a concluding remark regarding the activity of the synthesized catalyst since the reaction did not take place under the same conditions. This, however, does hint and support the potential of the Cu-Fe PILC to be applied as catalyst in the degradation of paracetamol.

3.5. Reaction intermediates in the paracetamol degradation by photo-Fenton process

Paracetamol molecule was readily degraded by photo-Fenton process catalyzed by a pillared clay containing both, Fe and Cu ions and at two different pH conditions (2.7 and 5.8) (see Fig. 3). In both cases, the total mineralization was not reached (see Fig. 4), and this might be due to the formation of recalcitrant intermediate products identified by HPLC-MS analysis (mainly acetamide). The effect of pH on the concentration profiles of the main reaction intermediates are plotted in Fig. 5. The main identified by-products were hydroquinone, acetamide and oxamic acid at both essayed pH conditions, while 1,2 Benzoquinone and 1,4 Benzoquinone were detected in less proportions only when H_2SO_4 0.1 M was added to the reactor to keep acidic conditions. Albeit other carboxylic acids were not observed, this does not necessarily mean that they are not produced. It might only be that its concentration is rather low to be quantified by the applied analytical technique. In any case, they are readily mineralized and the remaining TOC can be ascribed mainly to acetamide. Interestingly enough, after 180 min of degradation of paracetamol the concentrations of the main intermediates practically were the same for both cases, but the by-products degradation rate was slightly higher at pH near to 3.0. The maximum difference in final concentrations corresponds to oxamic acid and it was only 1.6 ppm. This fact implies that the performance of photo-Fenton process under conditions near to neutral pH is a promising alternative for the efficient degradation of organic pollutants without the necessity to keep acidic conditions along the entire process. Moreover, the formation and subsequent degradation of hydroquinone is clearly influenced by the pH and it is given by the noticeable differences in hydroquinone concentrations for both processes. Acetamide and oxamic acid exhibit a very similar behavior along of the experiment and while oxamic acid and hydroquinone practically are completely degraded (final concentration after 180 min is less than 5 ppm), disappearance of acetamide is considerably slow after 60 min of reaction and almost 30 ppm could not be eliminated under the reaction conditions essayed. Even though 30 ppm of acetamide are still in solution after a long period of reaction and may represent an important

Table 2
Paracetamol initial oxidation rates with different photochemical reaction systems.

Catalyst	Catalyst loading (mg L^{-1})	Paracetamol initial concentration (mg L^{-1})	[H_2O_2] (mg L^{-1})	Radiation wavelength (nm)	pH	$-r_{P,o}$ x10^7 (mol·L^{-1}·s^{-1})	$-r'_{P,o}$ (mol·g$_{cat}^{-1}$·s^{-1})	Reference
Cu/Fe-PILC	50	100	483	254	3	9.61	1.92×10^{-5}	This work
Cu/Fe-PILC	50	100	483	254	5.8	5.47	1.09×10^{-5}	This work
$FeSO_4$	2*	50	120	> 365	2-3	1.099	—	[9]
TiO_2	400	606	None	254	—	2.96	7.407×10^{-7}	[5]
Cu°, CuO	5000	50	None	None	3	2.198	4.397×10^{-8}	[49]

* This loading is given in mM since this is a homogeneous system (iron is ionized).

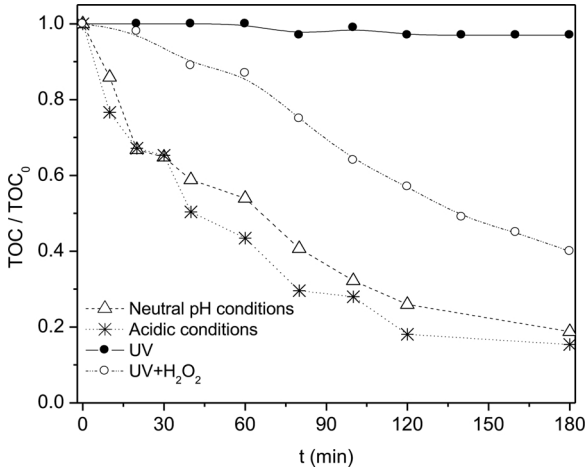

Fig. 4. Paracetamol normalized Total Organic Carbon-time profile by (a) Photolysis (UV), (b) UV + H_2O_2, (c) Photo-Fenton process catalyzed with Cu/Fe-pillared clay under different pH. Reaction conditions: TOC_0 = 64 mg L^{-1}, rpm = 800, T = 298 K, W_{cat} = 0.5 g L^{-1}, $V_{reaction}$ = 0.1 L.

drawback for the proposed technology. It has been reported that toxicity of the acetamide is considered low for animal species like fish, birds and insects and only in concentrations higher than 10,000 ppm acetamide could represent a danger for life of the mentioned species [50]. In a research conducted by Vel Leitner et al. [51], the oxidation of acetamide by OH radicals was investigated and among the studied variables, it was found that acetamide oxidation occurs more quickly in oxygen-free solutions. It is worth pointing out that this was not the case during the present investigation.

It has been previously stated that oxamic acid is a very recalcitrant compound towards advanced oxidation processes due to its low reactivity with hydroxyl radicals [52] and an additional relevant data is provided by Vel Leitner et al. [51] who mentioned that oxidation of oxamic acid by hydroxyl radicals may require about 100 times higher radicals amount than most organic compounds resulting in a difficult process. Contrasting with these reports, in our experiments oxamic acid did not show excessive resistance to its degradation likely helped for the appropriate conditions to produce OH radicals given by the catalytic properties of the pillared clays (Fig. 5B).

Based on the concentration profiles depicted in Fig. 5, there are three main reaction intermediates detected in this work and may be explained as follows: paracetamol undergoes oxidation initially through ·OH addition onto the aromatic ring in *para* position to produce hydroquinone and acetamide (see route [a], Fig. 6).

It has been reported that the additional oxidation of acetamide leads to the production of oxamic acid [51]. However, based on the evolution of oxamic acid over time (Fig. 5), it can be concluded that this is not the case. Furthermore, Vogna et al. [53] assessed the acetamide oxidation by UV and H_2O_2 and concluded this process does not lead to oxamic acid. Consequently, an alternative route for the observed production of oxamic acid is proposed and this is route [b] in Fig. 6. This route was established according to that reported by Vogna et al. that basically consists of the hydroxylation of the aromatic ring and then a muconic type cleavage due to an excess of OH radicals. Although in such study there is suggested the production of two types of acids, in this work, by LC–MS, only one could be observed that corresponded to the first intermediate in route [b]. It is worth pointing out that this compound was detected only during the first 5 min of reaction and therefore its concentration profile is not included. Nevertheless, in either route, [a] or [b], the mineralization of hydroquinone and oxamic acid is attained. As

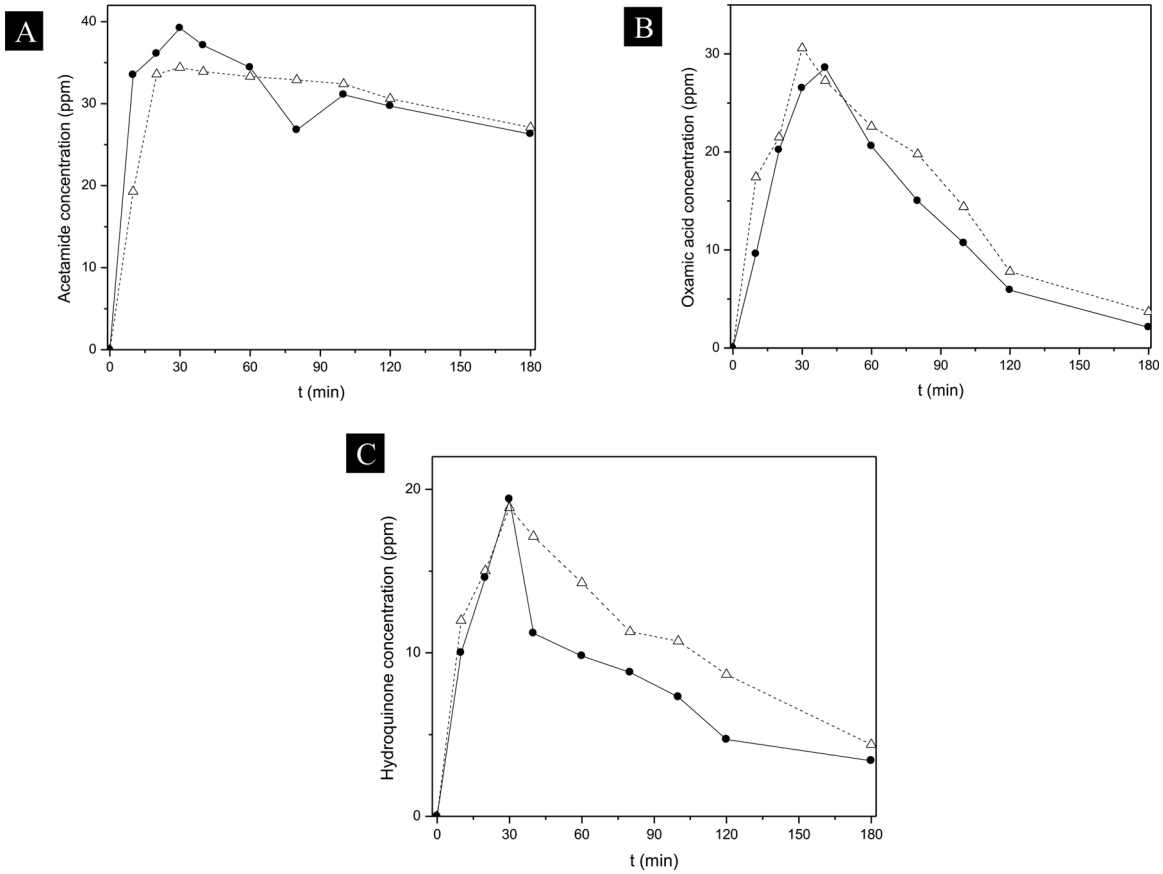

Fig. 5. Concentration profile of the paracetamol degradation by-products (A: Acetamide; B: Oxamic acid; C: Hydroquinone) detected in the following experiments: Cu/Fe-PILC circumneutral conditions (Δ) and Cu/Fe-PILC acidic conditions (●).

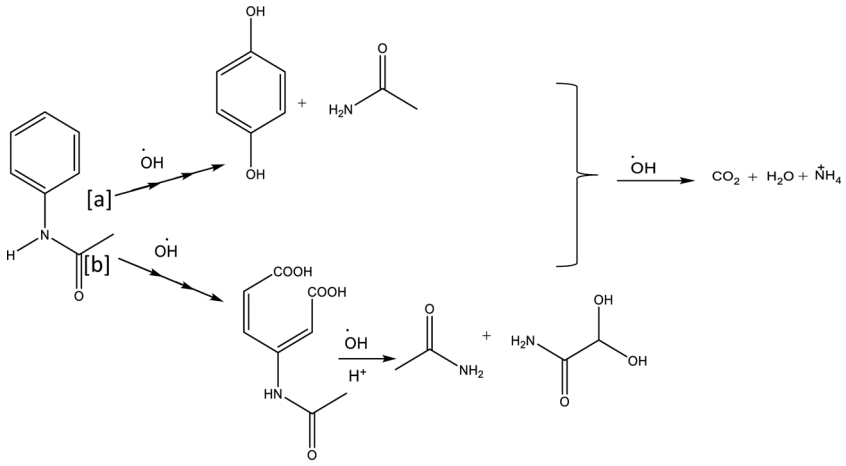

Fig. 6. Proposed reaction pathway for paracetamol oxidation via photo-Fenton process catalyzed with Cu-Fe-pillared clay (reaction time = 180 min).

aforementioned, the presence of carboxylic acids like oxalic, maleic and malonic were expected and for sure they were produced and rapidly oxidized to CO_2 and H_2O. This is worth pointing out since oxalic acid has been reported as a hard compound to be further oxidized. Furthermore, a collateral effect of the formation of hydroquinone as reaction intermediate is, according to Minella et al. investigations [11], that hydroquinone may help to reduce Fe^{3+} to Fe^{2+} which considerably accelerates the production of hydroxyl radicals in addition to the effect of light supplied to the system. In this sense, hydroquinone formation may result helpful to reach higher mineralization of organic pollutants.

3.6. Reusability of the Cu/Fe-PILC sample: a preliminary study

Cu/Fe-PILC powder was filtered from the reaction media, washed, dried and reused in a new photo-Fenton process for degradation of paracetamol maintaining the same operation conditions used for the first cycle under circumneutral pH conditions. The mineralization reached was also followed and after 120 min the mineralization was about 71% representing a loss of efficiency of only 3% with respect to the first cycle. This loss of efficiency can be ascribed to the leaching of 3.0% of initial iron content while Cu content was reduced in only 0.2%. This was established by atomic absorption measurements. Lixiviation or leaching of iron is a common phenomenon in catalysts employed for heterogeneous photo-Fenton and is strongly influenced by pH. For example, Ding et al. [54] concluded from their research on photo-Fenton that leaching of iron and copper from Cu-Fe bimetallic polytetrafluoroethylene complexes increases with a decrease in the solution pH. This result suggests that Cu/Fe-PILC reusability is promising. Thus, a more comprehensive study in this regard is desirable.

On the basis of the previous results of mineralization, stability of the catalyst and reusability, we may conclude that using Cu/Fe-PILC as catalyst in the oxidation of paracetamol by photo-Fenton process is beneficial since after 180 min of treatment, near of 80% of organic matter present at the beginning of the process was destroyed while the residual intermediate products not represent important toxicity to the environment and most important, the Fenton process may be conducted at natural pH of the solution without precipitation of iron species (by adding NaOH for example). On the other hand, it is desirable to minimize metals lixiviation from the catalyst and for our research group this fact represents an area of opportunity for the catalyst presented in this work due to its interesting performance for mineralization of organic pollutants at almost neutral pH.

4. Conclusions

Iron pillared clay (Fe-PILC) ion-exchanged with copper (Cu/Fe-PILC) was prepared. This clay, with a specific surface area of $110\ m^2\ g^{-1}$ and an Fe and Cu content of 16.49% and 4.04%, respectively, is a promising catalyst to conduct photo-Fenton processes since allows to conduct the mineralization of paracetamol at least twice faster than applying only UV light and H_2O_2 and it can be reused without compromising efficiency at circumneutral pH conditions. The phases responsible of the activity of the catalyst are FeO, Fe_3O_4, CuO and Cu_2O. After 180 min of reaction, the mineralization degree achieved under circumneutral pH conditions was about 80% only 2% below the mineralization degree attained at acidic conditions. The observed remained TOC corresponds mainly to the presence of acetamide which was not oxidized at the studied conditions. Nevertheless, highly toxic compounds like oxalic acid were totally removed and this is worth taken into account from an environmental point of view.

Acknowledgements

Financial support from CONACYT through project 269093 is greatly appreciated and R. Natividad is grateful to PRODEP for financial support (511-6/178590). A. Mendoza acknowledges CONACYT [scholarship 290817]. R. Romero acknowledges CONACYT financial support to conduct a sabbatical stay. Citlalit Martínez is acknowledged for technical support and Uvaldo Hernández for XRD analysis.

Appendix A. Supplementary data

Supplementary material related to this article can be found, in the online version, at doi:https://doi.org/10.1016/j.jphotochem.2019.01.012.

References

[1] L.H.M.L.M. Santos, A.N. Araújo, A. Fachini, A. Pena, C. Delerue-Matos, M.C.B.S.M. Montenegro, Ecotoxicological aspects related to the presence of pharmaceuticals in the aquatic environment, J. Hazard. Mater. 175 (2010) 45–95, https://doi.org/10.1016/j.jhazmat.2009.10.100.

[2] B. Nunes, S.C. Antunes, J. Santos, L. Martins, B.B. Castro, Toxic potential of paracetamol to freshwater organisms: a headache to environmental regulators? Ecotoxicol. Environ. Saf. 107 (2014) 178–185, https://doi.org/10.1016/j.ecoenv.2014.05.027.

[3] K.A. Novoa-Luna, A. Mendoza-Zepeda, R. Natividad, R. Romero, M. Galar-Martínez, L.M. Gómez-Oliván, Biological hazard evaluation of a pharmaceutical effluent before and after a photo-Fenton treatment, Sci. Total Environ. 569–570 (2016) 830–840, https://doi.org/10.1016/J.SCITOTENV.2016.06.086.

[4] E. De Laurentiis, C. Prasse, T.A. Ternes, M. Minella, V. Maurino, C. Minero, M. Sarakha, M. Brigante, D. Vione, Assessing the photochemical transformation pathways of acetaminophen relevant to surface waters: transformation kinetics,

intermediates, and modelling, Water Res. 53 (2014) 235–248, https://doi.org/10.1016/j.watres.2014.01.016.
[5] L. Yang, L.E. Yu, M.B. Ray, Photocatalytic oxidation of paracetamol: dominant reactants, intermediates, and reaction mechanisms, Environ. Sci. Technol. 43 (2009) 460–465, https://doi.org/10.1021/es8020099.
[6] E. Moctezuma, E. Leyva, C.A. Aguilar, R.A. Luna, C. Montalvo, Photocatalytic degradation of paracetamol: intermediates and total reaction mechanism, J. Hazard. Mater. 243 (2012) 130–138, https://doi.org/10.1016/j.jhazmat.2012.10.010.
[7] M.D.G. De Luna, M.L. Veciana, C.C. Su, M.C. Lu, Acetaminophen degradation by electro-Fenton and photoelectro-Fenton using a double cathode electrochemical cell, J. Hazard. Mater. 217–218 (2012) 200–207, https://doi.org/10.1016/j.jhazmat.2012.03.018.
[8] T.X.H. Le, T. Van Nguyen, Z. Amadou Yacouba, L. Zoungrana, F. Avril, D.L. Nguyen, E. Petit, J. Mendret, V. Bonniol, M. Bechelany, S. Lacour, G. Lesage, M. Cretin, Correlation between degradation pathway and toxicity of acetaminophen and its by-products by using the electro-Fenton process in aqueous media, Chemosphere 172 (2017) 1–9, https://doi.org/10.1016/j.chemosphere.2016.12.060.
[9] A.G. Trovó, R.F. Pupo Nogueira, A. Agüera, A.R. Fernandez-Alba, S. Malato, Paracetamol degradation intermediates and toxicity during photo-Fenton treatment using different iron species, Water Res. 46 (2012) 5374–5380, https://doi.org/10.1016/j.watres.2012.07.015.
[10] P.V. Nidheesh, Heterogeneous Fenton catalysts for the abatement of organic pollutants from aqueous solution: a review, RSC Adv. 5 (2015) 40552–40577, https://doi.org/10.1039/C5RA02023A.
[11] M. Minella, G. Marchetti, E. De Laurentiis, M. Malandrino, V. Maurino, C. Minero, D. Vione, K. Hanna, Photo-Fenton oxidation of phenol with magnetite as iron source, Appl. Catal. B Environ. 154–155 (2014) 102–109, https://doi.org/10.1016/j.apcatb.2014.02.006.
[12] S. Rahim Pouran, A.R. Abdul Aziz, W.M.A. Wan Daud, Review on the main advances in photo-Fenton oxidation system for recalcitrant wastewaters, J. Ind. Eng. Chem. 21 (2015) 53–69, https://doi.org/10.1016/j.jiec.2014.05.005.
[13] L.O. Conte, A.V. Schenone, O.M. Alfano, Photo-Fenton degradation of the herbicide 2,4-D in aqueous medium at pH conditions close to neutrality, J. Environ. Manage. 170 (2016) 60–69, https://doi.org/10.1016/J.JENVMAN.2016.01.002.
[14] V. Romero, S. Acevedo, P. Marco, J. Giménez, S. Esplugas, Enhancement of Fenton and photo-Fenton processes at initial circumneutral pH for the degradation of the β-blocker metoprolol, Water Res. 88 (2016) 449–457, https://doi.org/10.1016/J.WATRES.2015.10.035.
[15] S. Chen, Y. Wu, G. Li, J. Wu, G. Meng, X. Guo, Z. Liu, A novel strategy for preparation of an effective and stable heterogeneous photo-Fenton catalyst for the degradation of dye, Appl. Clay Sci. 136 (2017) 103–111, https://doi.org/10.1016/J.CLAY.2016.11.016.
[16] H. Dai, S. Xu, J. Chen, X. Miao, J. Zhu, Oxalate enhanced degradation of Orange II in heterogeneous UV-Fenton system catalyzed by Fe_3O_4@γ-Fe_2O_3 composite, Chemosphere 199 (2018) 147–153, https://doi.org/10.1016/J.CHEMOSPHERE.2018.02.016.
[17] I. Amildon Ricardo, C.E.S. Paniagua, V.A.B. Paiva, B.R. Gonçalves, R.M.F. Sousa, A.E.H. Machado, A.G. Trovó, Degradation and initial mechanism pathway of chloramphenicol by photo-Fenton process at circumneutral pH, Chem. Eng. J. 339 (2018) 531–538, https://doi.org/10.1016/J.CEJ.2018.01.144.
[18] M.A. De León, J. Castiglioni, J. Bussi, M. Sergio, Catalytic activity of an iron-pillared montmorillonitic clay mineral in heterogeneous photo-Fenton process, Catal. Today 133–135 (2008) 600–605, https://doi.org/10.1016/j.cattod.2007.12.130.
[19] H. Li, Y. Li, L. Xiang, Q. Huang, J. Qiu, H. Zhang, M.V. Sivaiah, F. Baron, J. Barrault, S. Petit, S. Valange, Heterogeneous photo-Fenton decolorization of Orange II over Al-pillared Fe-smectite: response surface approach, degradation pathway, and toxicity evaluation, J. Hazard. Mater. 287 (2015) 32–41, https://doi.org/10.1016/J.JHAZMAT.2015.01.023.
[20] F. Tomul, F. Turgut Basoglu, H. Canbay, Determination of adsorptive and catalytic properties of copper, silver and iron contain titanium-pillared bentonite for the removal bisphenol A from aqueous solution, Appl. Surf. Sci. 360 (2016) 579–593, https://doi.org/10.1016/J.APSUSC.2015.10.228.
[21] C. Catrinescu, D. Arsene, P. Apopei, C. Teodosiu, Degradation of 4-chlorophenol from wastewater through heterogeneous Fenton and photo-Fenton process, catalyzed by Al–Fe PILC, Appl. Clay Sci. 58 (2012) 96–101, https://doi.org/10.1016/J.CLAY.2012.01.019.
[22] H. Hassan, B.H. Hameed, Fenton-like oxidation of acid red 1 solutions using heterogeneous catalyst based on ball clay, Int. J. Environ. Sci. Dev. (2011) 218–222, https://doi.org/10.7763/IJESD.2011.V2.127.
[23] J. Herney-Ramirez, M.A. Vicente, L.M. Madeira, Heterogeneous photo-Fenton oxidation with pillared clay-based catalysts for wastewater treatment: a review, Appl. Catal. B Environ. 98 (2010) 10–26, https://doi.org/10.1016/j.apcatb.2010.05.004.
[24] A. Gil, S.A. Korili, R. Trujillano, M.A. Vicente, A review on characterization of pillared clays by specific techniques, Appl. Clay Sci. 53 (2011) 97–105, https://doi.org/10.1016/j.clay.2010.09.018.
[25] J. Feng, X. Hu, P.L. Yue, Effect of initial solution pH on the degradation of Orange II using clay-based Fe nanocomposites as heterogeneous photo-Fenton catalyst, Water Res. 40 (2006) 641–646, https://doi.org/10.1016/j.watres.2005.12.021.
[26] O.S.N. Sum, J. Feng, X. Hub, P.L. Yue, Photo-assisted fenton mineralization of an azo-dye acid black 1 using a modified laponite clay-based Fe nanocomposite as a heterogeneous catalyst, Top. Catal. 33 (2005) 233–242, https://doi.org/10.1007/s11244-005-2532-2.
[27] A.C.K. Yip, F.L.Y. Lam, X. Hu, Chemical-vapor-deposited copper on acid-activated bentonite clay as an applicable heterogeneous catalyst for the photo-fenton-like oxidation of textile organic pollutants, Ind. Eng. Chem. Res. 44 (2005) 7983–7990, https://doi.org/10.1021/ie050647y.
[28] K. Bahranowski, M. Gąsior, A. Kielski, J. Podobiński, E.M. Serwicka, L.A. Vartikian, K. Wodnicka, Copper-doped alumina-pillared montmorillonites as catalysts for oxidation of toluene and xylenes with hydrogen peroxide, Clay Miner. 34 (1999) 79–87, https://doi.org/10.1180/000985599546091.
[29] S. Caudo, G. Centi, C. Genovese, S. Perathoner, Homogeneous versus heterogeneous catalytic reactions to eliminate organics from waste water using H_2O_2, Top. Catal. 40 (2006) 207–219, https://doi.org/10.1007/s11244-006-0122-6.
[30] M.N. Timofeeva, S.T. Khankhasaeva, E.P. Talsi, V.N. Panchenko, A.V. Golovin, E.T. Dashinamzhilova, S.V. Tsybulya, The effect of Fe/Cu ratio in the synthesis of mixed Fe,Cu,Al-clays used as catalysts in phenol peroxide oxidation, Appl. Catal. B Environ. 90 (2009) 618–627, https://doi.org/10.1016/J.APCATB.2009.04.024.
[31] J. Barrault, C. Bouchoule, K. Echachoui, N. Frini-Srasra, M. Trabelsi, F. Bergaya, Catalytic wet peroxide oxidation (CWPO) of phenol over mixed (AlCu)-pillared clays, Appl. Catal. B Environ. 15 (1998) 269–274, https://doi.org/10.1016/S0926-3373(97)00054-4.
[32] Y. Zhang, Q. Zhang, Z. Dong, Wu liying, J. Hong, Degradation of acetaminophen with ferrous/copperoxide activate persulfate: synergism of iron and copper, Water Res. 146 (2018) 232–243, https://doi.org/10.1016/J.WATRES.2018.09.028.
[33] S. Minz, S. Garg, R. Gupta, Catalytic wet peroxide oxidation of 4-nitrophenol over Al–Fe, Al–Cu and Al–Cu–Fe pillared clays, Indian Chem. Eng. 60 (2018) 16–36, https://doi.org/10.1080/00194506.2016.1270780.
[34] Y. Zhang, J. Fan, B. Yang, W. Huang, L. Ma, Copper–catalyzed activation of molecular oxygen for oxidative destruction of acetaminophen: the mechanism and superoxide-mediated cycling of copper species, Chemosphere 166 (2017) 89–95, https://doi.org/10.1016/J.CHEMOSPHERE.2016.09.066.
[35] J.L. Valverde, A. Romero, R. Romero, P.B. García, M.L. Sánchez, I. Asencio, Preparation and characterization of Fe-PILCs. Influence of the synthesis parameters, Clays Clay Miner. 53 (2005) 613–621, https://doi.org/10.1346/CCMN.2005.0530607.
[36] A. Mendoza-Zepeda, Degradación de AINES mediante foto-Fenton, Universidad Autónoma del Estado de México, 2016 Master thesis (Accessed 6 June 2018) http://ri.uaemex.mx/handle/20.500.11799/65199.
[37] E. Martin Del Campo, R. Romero, G. Roa, E. Peralta-Reyes, J. Espino-Valencia, R. Natividad, Photo-Fenton oxidation of phenolic compounds catalyzed by iron-PILC, Fuel 138 (2014) 149–155, https://doi.org/10.1016/j.fuel.2014.06.014.
[38] M. Bernal, R. Romero, G. Roa, C. Barrera-Díaz, T. Torres-Blancas, R. Natividad, Ozonation of indigo carmine catalyzed with Fe-pillared clay, Int. J. Photoenergy 2013 (2013) 1–7, https://doi.org/10.1155/2013/918025.
[39] X. Li, G. Lu, Z. Qu, D. Zhang, S. Liu, The role of titania pillar in copper-ion exchanged titania pillared clays for the selective catalytic reduction of NO by propylene, Appl. Catal. A Gen. 398 (2011) 82–87, https://doi.org/10.1016/j.apcata.2011.03.020.
[40] F. Dorado, A. de Lucas, P.B. García, A. Romero, J.L. Valverde, Copper ion-exchanged and impregnated Fe-pillared clays. Study of the influence of the synthesis conditions on the activity for the selective catalytic reduction of NO with C_3H_6, Appl. Catal. A Gen. 305 (2006) 189–196, https://doi.org/10.1016/j.apcata.2006.03.022.
[41] F. Dorado, P.B. García, A. de Lucas, M.J. Ramos, A. Romero, Hydrocarbon selective catalytic reduction of NO over Cu/Fe-pillared clays: diffuse reflectance infrared spectroscopy studies, J. Mol. Catal. A Chem. 332 (2010) 45–52, https://doi.org/10.1016/J.MOLCATA.2010.08.019.
[42] L. Huang, F. Peng, H. Yu, H. Wang, Preparation of cuprous oxides with different sizes and their behaviors of adsorption, visible-light driven photocatalysis and photocorrosion, Solid State Sci. 11 (2009) 129–138, https://doi.org/10.1016/j.solidstatesciences.2008.04.013.
[43] C.Y. Kuo, C.H. Wu, J.T. Wu, Y.C. Chen, Preparation of immobilized Cu_2O using microwave irradiation and its catalytic activity for bisphenol A: comparisons of Cu_2O/H_2O_2 and visible-light/Cu_2O/H_2O_2 systems, Water Sci. Technol. 70 (2014) 1428, https://doi.org/10.2166/wst.2014.373.
[44] T. Undabeytia, M.C. Galán-Jiménez, E. Gómez-Pantoja, J. Vázquez, B. Casal, F. Bergaya, E. Morillo, Fe-pillared clay mineral-based formulations of imazaquin for reduced leaching in soil, Appl. Clay Sci. 80–81 (2013) 382–389, https://doi.org/10.1016/j.clay.2013.07.001.
[45] R.Q. Long, R.T. Yang, Catalytic performance and characterization of VO^{2+}-exchanged titania-pillared clays for selective catalytic reduction of nitric oxide with ammonia, J. Catal. 196 (2000) 73–85, https://doi.org/10.1006/JCAT.2000.3015.
[46] K. Bahranowski, R. Dula, M. Łabanowska, E.M. Serwicka, ESR study of Cu centers supported on Al-, Ti-, and Zr-pillared montmorillonite clays, Appl. Spectrosc. 50 (1996) 1439–1445, https://doi.org/10.1366/0003702963904809.
[47] M. Thommes, K. Kaneko, A.V. Neimark, J.P. Olivier, F. Rodriguez-Reinoso, J. Rouquerol, K.S.W. Sing, Physisorption of gases, with special reference to the evaluation of surface area and pore size distribution (IUPAC Technical Report), Pure Appl. Chem. 87 (2015) 1051–1069, https://doi.org/10.1515/pac-2014-1117.
[48] J.G. Carriazo, Influence of iron removal on the synthesis of pillared clays: a surface study by nitrogen adsorption, XRD and EPR, Appl. Clay Sci. 67–68 (2012) 99–105, https://doi.org/10.1016/J.CLAY.2012.07.010.
[49] Y. Zhang, J. Fan, B. Yang, W. Huang, L. Ma, Copper–catalyzed activation of molecular oxygen for oxidative destruction of acetaminophen: the mechanism and superoxide-mediated cycling of copper species, Chemosphere 166 (2017) 89–95, https://doi.org/10.1016/j.chemosphere.2016.09.066.
[50] G.L. Kennedy, R.D. Short, Biological effects of acetamide, formamide, and their monomethyl and dimethyl derivatives, CRC Crit. Rev. Toxicol. 17 (1986) 129–182, https://doi.org/10.3109/10408448609023768.
[51] N. Karpel Vel Leitner, P. Berger, B. Legube, Oxidation of amino groups by hydroxyl radicals in relation to the oxidation degree of the α-carbon, Environ. Sci. Technol. 36 (2002) 3083–3089, https://doi.org/10.1021/es0101173.

[52] S. Fleischer, S.C. Weiss, T. Lucke, W. Seitz, W. Schulz, W.H. Weber, Formation of oxamic acid during drinking water treatment, Ozone Sci. Eng. 37 (2015) 441–449, https://doi.org/10.1080/01919512.2015.1040911.
[53] D. Vogna, R. Marotta, A. Napolitano, M. D'Ischia, Advanced oxidation chemistry of paracetamol. UV/H_2O_2-induced hydroxylation/degradation pathways and 15N-aided inventory of nitrogenous breakdown products, J. Org. Chem. 67 (2002) 6143–6151, https://doi.org/10.1021/jo025604v.
[54] Z. Ding, Y. Dong, B. Li, Preparation of a modified PTFE fibrous photo-fenton catalyst and its optimization towards the degradation of organic dye, Int. J. Photoenergy 2012 (2012) 1–8, https://doi.org/10.1155/2012/121239.